

PCCP

Accepted Manuscript



This is an *Accepted Manuscript*, which has been through the Royal Society of Chemistry peer review process and has been accepted for publication.

Accepted Manuscripts are published online shortly after acceptance, before technical editing, formatting and proof reading. Using this free service, authors can make their results available to the community, in citable form, before we publish the edited article. We will replace this *Accepted Manuscript* with the edited and formatted *Advance Article* as soon as it is available.

You can find more information about *Accepted Manuscripts* in the [Information for Authors](#).

Please note that technical editing may introduce minor changes to the text and/or graphics, which may alter content. The journal's standard [Terms & Conditions](#) and the [Ethical guidelines](#) still apply. In no event shall the Royal Society of Chemistry be held responsible for any errors or omissions in this *Accepted Manuscript* or any consequences arising from the use of any information it contains.

Delocalized Quantum States Enhance Photocell Efficiency

Yiteng Zhang^{a,b}, Sangchul Oh,^a Fahhad H. Alharbi,^a Greg Engel,^c and Sabre Kais^{a,b,*}

Received January 16, 2015,

The high quantum efficiency of photosynthetic complexes has inspired researchers to explore new routes to utilize this process for photovoltaic devices. Quantum coherence has been demonstrated to play a crucial role within this process. Herein, we propose a three-dipole system as a model of a new photocell type which exploits the coherence among its three dipoles. We have proved that the efficiency of such a photocell is greatly enhanced by quantum coherence. We have also predicted that the photocurrents can be enhanced by about 49.5% in such a coherent coupled dipole system compared with the uncoupled dipoles. These results suggest a promising novel design aspect of photosynthesis-mimicking photovoltaic devices.

1 Introduction

Long-lived quantum coherence has been observed in photosynthesis after laser excitation^{1–7}. It has attracted much attention on how quantum coherence could be enhanced in complex biological environment and how it may play a key role in efficient exciton transports^{8–12}. It is well known that the photon-to-charge conversion quantum efficiency of photosynthesis in plants, bacteria, and algae can be almost 100% under certain conditions. While photosynthesis converts sunlight into chemical energy, solar cell converts sunlight into electric energy. According to Shockley and Queisser, the efficiency of photovoltaic energy conversion is limited to 33%, based on the energy band gap and solar spectrum, due to the radiative recombination of electron-hole pairs, thermalization, and unabsorbed photons¹³. Various attempts have been made to improve the performance of photovoltaic devices^{14–18}. Mimicking photosynthesis presents a promising route by which to increase the efficiency of the current solar cell technology¹⁹. Consequently, there has been a long-standing and increasing interest in the understanding of the physics describing the energy conversion within photosynthesis. Recently, quantum coherence has demonstrated its crucial role in the energy conversion during photosynthesis^{1–12}. Similarly, it has been shown that quantum coherence can be used to alter the conditions of the detailed balance and thereby enhance the quantum efficiency in photocell^{20–25}. In principle, the Shockley-Queisser model is a two-extended-level model. By incorporating more levels and tuning them carefully, the conversion efficiency can be improved.

Recently, Creatore *et al.*²⁴ have shown that the delocal-

ized quantum state is capable of improving the photocurrent of a photocell by at least 35% in compared with a photocell with the localized quantum state when treating the photon-to-charge conversion as a continuous Carnot-like cycle²⁶. Within their model, the two delocalized states, called the bright and dark states, of the dipole-dipole interacting two donors play a key role in improving the efficiency of the PV cell. Due to the constructive interference, the optical transition rate between the ground and the bright states becomes two times stronger than the uncoupled donor case. While it is blocked through the bright state due to the destructive interference, the electron transition from the excited donor to the acceptor is made only through the dark state and its rate is two times larger than the uncoupled donor case, due to the constructive interference. Consequently, the presence of quantum coherence of the delocalized donor states alters the conditions for the thermodynamic detailed balance; that results in the enhancement of the efficiency of the photocell.

In this paper, we show that a photocell with three suitably arranged electron donors coupled via dipole-dipole interactions can result in an enhancement of photocurrents by about 49.5% over a classical photocell. While inspired by Creatore *et al.*²⁴, our three coupled donors, rather than the two coupled ones, makes another big improvement in the efficiency of a PV cell. The origin of the photocurrent enhancement is explained by the key roles of the delocalized excited states of the donor system. The dipole-dipole coupling between donors make three degenerate and localized one-exciton levels split into three delocalized levels: the bright, almost-dark, and dark states. The photon absorption and emission rates between the ground and the bright excited state becomes about 2.91 times larger than that of the uncoupled donor case, which is due to the constructive interference of three donors. While the electron transferring from the donor to the acceptor through the almost-dark state is enhanced by about 2.91 times compared to the uncoupled donor case, but is almost blocked through

^a Qatar Environment and Energy Research Institute, Qatar Foundation, Doha, Qatar

^b Department of Chemistry, Physics and Birck Nanotechnology Center, Purdue University, West Lafayette, IN 47907 USA

^c Department of Chemistry, University of Chicago, Chicago, IL, 60637 USA

* Corresponding author; Email:kais@purdue.edu

the bright state, which are also due to the constructive and destructive interferences of the delocalized donor states. Basically, essential physics of our triple-donor model is similar to that of Creatore *et al.*'s two donor model, but more enhanced by collective properties. While it seems challenging, our proposed model could be realized by nanotechnologies inspired by natural light-harvesting structures.

2 PV Models with Two Donors

Before introducing a photovoltaic cell model with three donors, we discuss in detail how a configuration of two dipoles affects the efficiency of a PV cell in Creatore *et al.*'s model²⁴. The excitation of a molecule is simply modeled as a two-level system with the ground state $|b\rangle$ and excited state $|a\rangle$. The optical transition between them is characterized by the optical dipole moment $\mu = e\langle a|\mathbf{r}|b\rangle$. For a molecular aggregate composed of electric neutral molecules, the intermolecular interaction is given by the electrostatic dipole-dipole coupling³

$$J_{12} = \frac{1}{4\pi\epsilon\epsilon_0} \left(\frac{\boldsymbol{\mu}_1 \cdot \boldsymbol{\mu}_2}{r^3} - \frac{3(\boldsymbol{\mu}_1 \cdot \mathbf{r})(\boldsymbol{\mu}_2 \cdot \mathbf{r})}{r^5} \right), \quad (1)$$

where dipole moment $\boldsymbol{\mu}_1$ is located at \mathbf{r}_1 , $\boldsymbol{\mu}_2$ at \mathbf{r}_2 , and $\mathbf{r} = \mathbf{r}_2 - \mathbf{r}_1$ is the radius vector from $\boldsymbol{\mu}_1$ to $\boldsymbol{\mu}_2$. Typically, the strength of J_{12} is much weaker than the excitation energy $\hbar\omega = E_a - E_b$. The exciton dynamics of the aggregate is described by Hamiltonian²⁷

$$H = \sum_i \hbar\omega_i \sigma_i^+ \sigma_i^- + \sum_{i \neq j} J_{ij} (\sigma_i^- \sigma_j^+ + h.c.) \quad (2)$$

where $\sigma^+ = |a\rangle\langle b|$ and $\sigma^- = |b\rangle\langle a|$ are the Pauli raising and lowering operators, respectively.

According to Eq. (1) the strength of J_{12} depends on how dipole moments are aligned. In Creatore *et al.*'s paper²⁴, the donor is a dimer where the dipole moment $\boldsymbol{\mu}_1$ is always perpendicular to the radius vector \mathbf{r} so the second term in Eq. (1) vanishes. The dipole-dipole coupling is given by $J_{12} \propto \boldsymbol{\mu}_1 \cdot \boldsymbol{\mu}_2 = \mu_1 \mu_2 \cos \theta$ with angle θ between two dipole moments. This gives rise to the simple angle-dependence energy gap $\Delta E = 2J_{12}^0 |\cos \theta|$ between the symmetric and antisymmetric excited states. The spontaneous decay rates are also proportional to $|\mu|^2(1 \pm \cos \theta)$.

Molecules in aggregates, however, are more probable to be aligned collectively, not independently. We study how the H and J-aggregate donor alignments affect the efficiency of PV cells. As illustrated in Fig. 1, we consider the two dipole moments tilted at the same angle θ with respect to the vertical axis. The angle dependence of the dipole-dipole coupling of Eq. (1) becomes

$$J_{12}(\theta) = J_{12}^0 (1 - 3 \cos^2(\frac{\pi}{2} - \theta)). \quad (3)$$

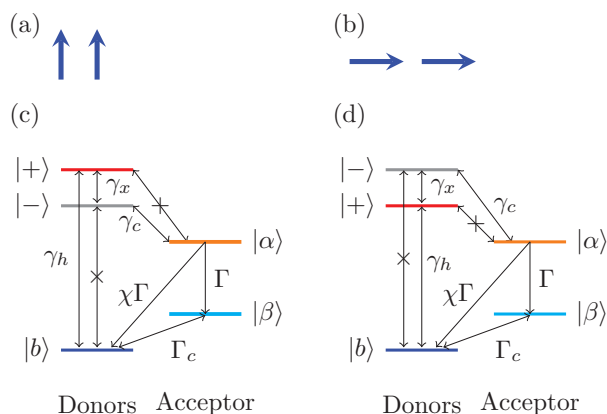


Fig. 1 Alignments of two dipole moments for (a) H-aggregate and (b) J-aggregate. Energy level diagrams and electron transition paths of (c) H-aggregate and (d) J-aggregate. The symmetric state $|+\rangle$ is optically bright and has the absorption and emission rate γ_h , but has no electron transition channel to the donor. The antisymmetric state $|-\rangle$ is dark but has the electron transfer path to the donor. The electron transition rate γ_x between the bright state $|+\rangle$ and dark state $|-\rangle$ is caused by thermal phonons.

This implies the angle dependence of the Davydov energy splitting $\Delta E(\theta) = 2|J_{12}(\theta)|$ between the symmetric and antisymmetric states. Also it explains the transition between the H-aggregate and the J-aggregate at the magic angle $\theta_c = \cos^{-1}(\frac{1}{\sqrt{3}}) \approx 54.74^\circ$ when the angle is measured from \mathbf{r} . Here the angle is measured with respect to the vertical axis so one has the magic angle $\theta_c \approx 35.26^\circ$ as shown in Fig. 2.

In contrast to Creatore *et al.*'s configuration, the symmetric state $|+\rangle = \frac{1}{\sqrt{2}}(|a_1\rangle + |a_2\rangle)$ in our model is always an optically active state (bright state)²⁸. For angles less than θ_c , this level is higher than the antisymmetric (dark) state $|-\rangle = \frac{1}{\sqrt{2}}(|a_1\rangle - |a_2\rangle)$ so the optical transition is shifted to the blue (H-aggregate). On the other hand, for angles greater than θ_c , the antisymmetric state is higher so the optical transition is changed to the red (J-aggregate). Note that classically the total dipole moment is always $2|\mu|$ because the two dipole moments point to the same direction. The dipole matrix element between the ground and bright states is $\sqrt{2}|\mu|$ so the optical transition rate γ_h , proportional to the square of the dipole matrix element, becomes doubled, i.e. $\gamma_h = 2\gamma_{1h}$, in compared with an uncoupled donor case. We calculate how the current enhancement is dependent on the angle θ , as plotted in Fig. 2. The two energy levels E_\pm for the symmetric and antisymmetric states move to $(E_a - E_b)/2$ as the angle θ increases. This affects the Bose-Einstein distributions, n_h of thermal photons, n_x and n_c of thermal phonon through the gaps $E_+ - E_b$, $E_+ - E_-$, and $E_\pm - E_\alpha$, respectively. Because of $(E_a - E_b) \gg J$, the distribution n_h is dependent

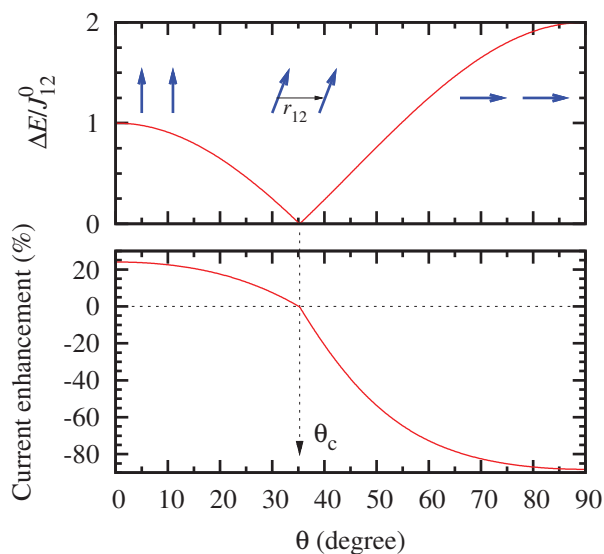


Fig. 2 (a) The energy gap ΔE between the bright and dark states and (b) the current enhancement as a function of the tilt angle θ with respect to the vertical axis. In (a) the alignment of two dipole moments is shown as the blue arrows. The two parallel dipole moments are aligned in head to head manner (H-aggregate) at $\theta = 0$ and in head to tail manner (J-aggregate) at $\theta = \pi/2$. In (b) the black arrow points to the magic angle $\theta_c \approx 35.26^\circ$.

little on the angle θ . However, n_x and n_c are strongly affected by the angle θ so drastic changes in current enhancement. For H-aggregate case ($\theta < \theta_c$), n_x increases but n_c decreases as angle θ increases. So the current enhancement decreases as angle θ increases. For J-aggregate case ($\theta > \theta_c$), the bright state is lower than the dark state. An electron in the bright state jumps to the dark state via only the absorption γ_x of thermal phonons (in H-aggregate case, the transition from the bright to dark states can be done via the stimulated emission and spontaneous emission of thermal phonons, $\gamma_x(1 + n_x)$). Thus, the transition from the donor to acceptor is very low, and the current enhancement is negative as shown in Fig. 2. In our model as well as Creatore *et al.*'s model²⁴, two donors are coupled to the acceptor so the bright state has no electron transferring channel to the acceptor because of the destructive interference. If a donor system is composed of many molecules (for example a linear chain), it is likely that only some donor molecules (or the molecules at the end site) are coupled to the acceptor so the transition path of the bright state to the donor would not be blocked.

3 PV model with three dipole donors

3.1 Model

The photocell model, proposed here, is depicted in Fig. 3. The picture of a classical cyclic engine is described as the following: D_1 , D_2 , and D_3 represent three identical and initially uncoupled donor molecules which are aligned around an acceptor molecule A . Initially, the system starts in the ground state $|b\rangle$. The cycle of electron transport begins with the absorption of solar photons populating the uncoupled donor excited states $|a_1\rangle$, $|a_2\rangle$, and $|a_3\rangle$. Then the excited electrons can be transferred to the acceptor molecule, the charge-separated state $|\alpha\rangle$, with any excess energy radiated as a phonon. The excited electron is then assumed to be used to perform work, leaving the charge-separated state $|\alpha\rangle$ decaying to the substable state $|\beta\rangle$. The recombination between the acceptor and the donor is also considered with a decay rate of $\Gamma_{\alpha \rightarrow b} = \chi\Gamma$, where χ is a dimensionless fraction. This loss channel brings the system back into the ground state without producing a work current, which could be a significant source of inefficiency. Finally, the state $|\beta\rangle$ decays back to the charge neutral ground state, closing the cycle. If considering the quantum effects resulting from the long-range dipole-dipole interaction, the new element of the system is the formation of new optically excitable states through strong exciton coupling among the donor molecules²⁴.

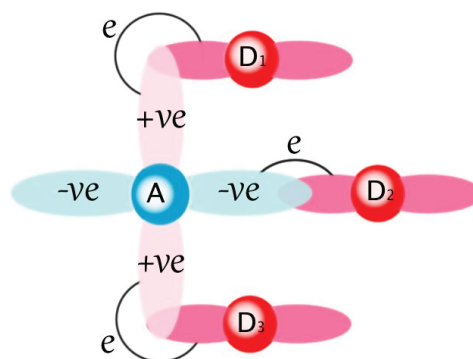


Fig. 3 Schematics of our PV cell. Three optically active donors, denoted by D_1 , D_2 , D_3 , become excited by absorbing incident photons and their excited electrons are transferred to the acceptor A . The pink and blue shadowed regions surrounding the molecules represent the molecular orbitals representing the spatial distribution of electron density.

For simplicity, we assume that three donors (D_1 , D_2 and D_3) are identical and degenerate, so the uncoupled excited states $|a_1\rangle$, $|a_2\rangle$ and $|a_3\rangle$ of the three donors have the same excitation levels $E_1 = E_2 = E_3 = \hbar\omega$. Furthermore, their dipole moments are aligned to the same direction, $\mu_1 = \mu_2 =$

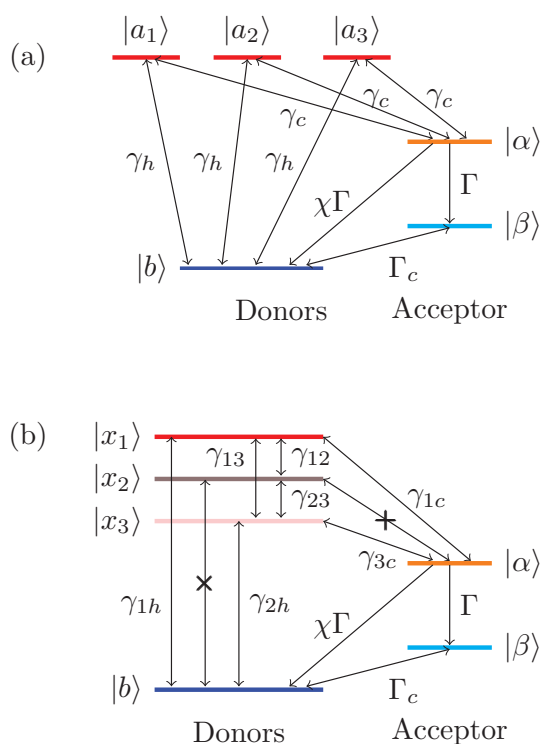


Fig. 4 Energy levels of the PV models (a) with the acceptor and three uncoupled donors and (b) with the acceptor and three dipole-dipole coupled donors. Black arrows indicate possible electron-transition paths. In (a) all the three donors are uncoupled and identical so have the same excitation energies (E_i), the same the photon absorption and emission rates γ_h between the ground state $|b\rangle$ and excited states $|a_i\rangle$, and the same electron transfer rates γ_c between the excited donors ($|a_i\rangle$) and the acceptor ($|\alpha\rangle$). In (b) due to the dipole-dipole couplings between three donors, the three degenerate excited levels in (a) become split, denoted by $|x_i\rangle$. The dark level ($|x_2\rangle$) is optically forbidden and has no electron transfer path to the donor ($|\alpha\rangle$).

$\mu_3 = \mu$ as depicted in Fig. 3. We assume the dipole-dipole interaction between only nearest neighbors. The dipole-dipole couplings between D_1 and D_2 , and D_2 and D_3 are denoted by J , but there is no coupling between D_1 and D_3 . The Hamiltonian for the system of three interacting donors is written as

$$H = \sum_{i=1}^3 \hbar\omega\sigma_i^+\sigma_i^- + J(\sigma_1^-\sigma_2^+ + \sigma_2^-\sigma_3^+ + h.c.). \quad (4)$$

It is straightforward to obtain the three single-excitation states of Hamiltonian (4): $|x_1\rangle = \frac{1}{2}(|a_1\rangle + \sqrt{2}|a_2\rangle + |a_3\rangle)$, $|x_2\rangle = \frac{1}{\sqrt{2}}(|a_1\rangle - |a_3\rangle)$, and $|x_3\rangle = \frac{1}{2}(|a_1\rangle - \sqrt{2}|a_2\rangle + |a_3\rangle)$. The corresponding eigenvalues are obtained as $E_{x_1} = E + \sqrt{2}J$, $E_{x_2} = E$, and $E_{x_3} = E - \sqrt{2}J$.

The dipole moment between the state $|x_1\rangle/|x_3\rangle$ and the

ground state $|0\rangle$ is enhanced/weakened by constructive interference between the individual transition dipole matrix elements, $\mu_{x_1/0} = \frac{1}{2}(\mu_1 \pm \sqrt{2}\mu_2 + \mu_3) = (1 \pm \frac{1}{\sqrt{2}})\mu$, while the dipole moment of the state $|x_2\rangle$ cancels due to destructive interference. This means the state $|x_2\rangle$, comprised of the antisymmetric combination of the uncoupled $|a_1\rangle$ and $|a_3\rangle$ states, describes an optically forbidden dark state. On the contrary, the $|x_1\rangle$ and $|x_3\rangle$ states describe two optically active bright states with photon absorption and emission rates $\gamma_{1h} \propto |\mu_{x_1}|^2 = (\frac{3}{2} + \sqrt{2})|\mu|^2$ and $\gamma_{3h} \propto |\mu_{x_3}|^2 = (\frac{3}{2} - \sqrt{2})|\mu|^2$, respectively, in compared with the uncoupled case, $\gamma_h \propto |\mu|^2$. In other words, $|x_1\rangle$ is much brighter than $|x_3\rangle$, as the photon absorption and emission rate of $|x_1\rangle$ is enhanced while that of $|x_3\rangle$ is weakened. Obviously, the dark state $|x_2\rangle$ has a resultant charge transfer matrix element equal to zero.

The intermolecular dipole interaction will also modify the transition rate between the donors and acceptor. The electron transfer matrix elements leading to charge separation have been chosen to have the same magnitudes $|t_{D_1A}| = |t_{D_2A}| = |t_{D_3A}| = t$. Also, we assume that the acceptor molecule hosts an electron within its lowest unoccupied molecular orbital, which is characterized by the shape of the d -orbitals (See Fig. 3). We have also assumed that the donor molecules are located close to different lobes of the acceptor molecular orbital; this leads to electron transfer matrix elements with the same magnitudes but different signs, i.e., $t_{D_1A} = -t_{D_2A} = t_{D_3A} = t$. Due to effects of the dipole-dipole interactions, the eigenstates of the three optically excited donors are no longer uncoupled, but are coherent exciton states. The bright states $|x_1\rangle/|x_3\rangle$ have matrix elements $t_{x_1A/x_3A} = \frac{1}{2}(t_{D_1A} \mp \sqrt{2}t_{D_2A} + t_{D_3A}) = (1 \mp \frac{1}{\sqrt{2}})t$, giving decreased/enhanced electron transfer rates of $\gamma_{1c/3c} \propto |t_{x_1A/x_3A}|^2 = (\frac{3}{2} \mp \sqrt{2})|t|^2$, in compared with the uncoupled case $\gamma_c \propto |t|^2$. These modifications of electron transfer matrix elements play a crucial role in the enhancement of photocurrents within our photocell model. The assumptions surrounding the electron transfer matrix elements is identical to that in Ref.²⁴.

Another crucial procedure in our model is phonon-mediated energy relaxation, which can be very effective between exciton states with strong pigment overlap^{24,29}. These relaxations are included in our kinetic model via the relaxation rates $\gamma_{12}, \gamma_{13}, \gamma_{23}$. Assuming that the new donor states are directly populated by the absorption of weak incoherent solar photons, the kinetics of the optically excited states obey the Pauli master equation (PME) by treating the donor-light, electron transfer, and bright-dark relaxation coupling by second-order perturbations²⁴.

The PME for the uncoupled case, describing the processes

as shown in Fig. 4 (a), are written as

$$\begin{aligned}\dot{p}_1 &= \gamma_h[n_h p_b - (1 + n_h)p_1] + \gamma_c[n_c p_\alpha - (1 + n_c)p_1], \\ \dot{p}_2 &= \gamma_h[n_h p_b - (1 + n_h)p_2] + \gamma_c[n_c p_\alpha - (1 + n_c)p_2], \\ \dot{p}_3 &= \gamma_h[n_h p_b - (1 + n_h)p_3] + \gamma_c[n_c p_\alpha - (1 + n_c)p_3], \\ \dot{p}_\alpha &= \gamma_c(1 + n_c)(p_1 + p_2 + p_3) - 3\gamma_c n_c p_\alpha - \Gamma(1 + \chi)p_\alpha, \\ \dot{p}_\beta &= \Gamma_c[N_c p_b - (1 + N_c)p_\beta] + \Gamma p_\alpha\end{aligned}\quad (5)$$

where we use the notation $p_i = \rho_{i,i}$ with indices i running as $b, 1 = a_1, 2 = a_2, 3 = a_3, \alpha, \beta$. Similarly, the PMEs for the dipole-dipole coupled case, whose processes are shown in Fig. 4 (b), are given by

$$\begin{aligned}\dot{p}_1 &= \gamma_{1h}[n_{1h}p_b - (1 + n_{1h})p_1] + \gamma_{12}[n_{12}p_2 - (1 + n_{12})p_1] \\ &\quad + \gamma_{13}[n_{13}p_3 - (1 + n_{13})p_1] + \gamma_{1c}[n_{1c}p_\alpha - (1 + n_{1c})p_1], \\ \dot{p}_2 &= \gamma_{12}[(1 + n_{12})p_1 - n_{12}p_2] + \gamma_{23}[n_{23}p_3 - (1 + n_{23})p_2], \\ \dot{p}_3 &= \gamma_{3h}[n_{3h}p_b - (1 + n_{3h})p_3] + \gamma_{23}[(1 + n_{23})p_2 - n_{23}p_3] \\ &\quad + \gamma_{13}[(1 + n_{13})p_1 - n_{13}p_3] + \gamma_{3c}[n_{3c}p_\alpha - (1 + n_{3c})p_3], \\ \dot{p}_\alpha &= \gamma_{1c}[(1 + n_{1c})p_1 - n_{1c}p_\alpha] + \gamma_{3c}[(1 + n_{3c})p_3 - n_{3c}p_\alpha] \\ &\quad - \Gamma(1 + \chi)p_\alpha, \\ \dot{p}_\beta &= \Gamma p_\alpha + \Gamma_c[N_c p_b - (1 + N_c)p_\beta],\end{aligned}\quad (6)$$

where index i of p_i runs as $b, 1 = x_1, 2 = x_2, 3 = x_3, \alpha, \beta$. In Eqs. (5) and (6), the equation of motion for $p_b = \rho_{bb}$ is determined by the conservation of the probability, $\sum_i p_i = \sum_i \rho_{ii} = 1$. In Eqs. (5) and (6), n_h and n_{1h} (n_{3h}) stand for the average numbers of photons with frequencies matching the transition energies from the ground state $|b\rangle$ to the excited states $|a_i\rangle$ and $|x_1\rangle$ ($|x_3\rangle$), respectively. n_c and n_{1c} (n_{3c}) are the thermal occupation numbers of ambient phonons at room temperature, $T_a = 300$ K, with energies $E - E_\alpha$ in Eq. (5) and $E_{x_1} - E_\alpha$ ($E_{x_3} - E_\alpha$) in Eq. (6). n_{12} , n_{13} , and n_{23} represent the corresponding thermal occupations at T_a with energies $E_{x_1} - E_{x_2}$, $E_{x_1} - E_{x_3}$, and $E_{x_2} - E_{x_3}$, respectively. N_c is the corresponding thermal occupation at T_a with the energy $E_\beta - E_b$. The rates in Eqs. (5) and (6) obey local detailed balance and correctly lead to a Boltzmann distribution for the level population if the thermal averages for the photon and phonon reservoirs are set to a common temperature, such as room temperature. We consider the initial condition to be a fully occupied ground state, i.e., $\rho_{bb}(t = 0) = 1$.

3.2 Results

To calculate the population of each state, we use the following parameters^{20,23,24}. The energy levels are $E - E_b = 1.8$ eV,

$E - E_\alpha = E_\beta - E_b = 0.2$ eV, and $J_{12} = J_{23} = J = 0.015$ eV. The transfer rates are taken as $\gamma_h = 0.62 \times 10^{-6}$ eV, $\gamma_c = 6$ meV, $\Gamma = 0.12$ eV, and $\Gamma_c = 0.025$ eV. We assume that the superposition states are stable under the steady-state operation, so that $\gamma_{13}, \gamma_{12}, \gamma_{23}$ have to satisfy the relationship: $\gamma_{13} = 2\gamma_{12} = 2\gamma_{23} \leq 2\sqrt{2}J$ ³⁰. Here, we choose as a limiting condition: $\gamma_{13} = 2\gamma_{12} = 2\gamma_{23} = 2\sqrt{2}J$. We also employed this as a limiting condition for Creator *et al.*'s model, to create an appropriate comparison with our model. Figs. 5 (a) and (b) show the populations of each state in the absence and presence of coupling. Due to the dipolar interaction among donors, the populations of the donors' ground state, $|b\rangle$, is significantly decreased while the populations of the acceptors' states, $|\alpha\rangle$ and $|\beta\rangle$, are notably increased in the presence of coherence when the system reaches the steady-state operation. These changes are responsible for the enhanced photocurrents.

We would like to emphasize that our model as well as Creator *et al.*'s²⁴ solves the Pauli master equation for the diagonal components $p_i = \rho_{i,i}$, but not for the off-diagonal components $\rho_{i,j}$ ($i \neq j$) of the density operator. The quantum coherence between delocalized excited donor states, represented by the off-diagonal components such as ρ_{x_1, x_2} , does not play the key role in increasing the efficiency of the solar cell. The enhancement comes from the large optical transition rate between the ground level b and the excited level x_1 , the forbidden transition between the ground level b and the excited level x_2 , and the constructive and destructive paths between the donor and acceptor. One may think the dephasing of each delocalized state. For example, when $|x_1\rangle$ becomes mixed, it will be the mixture of three bare states, $|a_1\rangle$, $|a_2\rangle$ and $|a_3\rangle$. The diagonal component $p_{x_1} = \rho_{x_1, x_1}$ can be expressed in terms of the diagonal and off-diagonal components with the bare states $\rho_{x_1, x_1} = \frac{1}{4}[\rho_{a_1, a_1} + 2\rho_{a_2, a_2} + \rho_{a_3, a_3} + 2\sqrt{2}\text{Re}(\rho_{a_1, a_2}) + 2\text{Re}(\rho_{a_1, a_3}) + 2\sqrt{2}\text{Re}(\rho_{a_2, a_3})]$. For a mixed state x_1 , it becomes

$$\bar{\rho}_{x_1, x_1} = \frac{1}{4}(\rho_{a_1, a_1} + 2\rho_{a_2, a_2} + \rho_{a_3, a_3}). \quad (7)$$

However, the energy for the mixed state $E = \text{Tr}(H\bar{\rho}_{x_1, x_1})$ becomes just $\hbar\omega$ of the uncoupled donor, not $\hbar\omega + \sqrt{2}J$ for the energy level of the coupled one. Thus as long as the coupling between donor molecules is strong enough, the excited energy levels are well defined and the delocalized states are in a pure state as we assume.

In the quantum heat engine model of a solar cell, the acceptor's states $|\alpha\rangle$ and $|\beta\rangle$ represent the conduction band α of a cathode and the valence band β of an anode. The resistance of an external load connected to them is characterized by the decay rate Γ of electrons from α to β . The current flows from the lead β to α and is given by $j = e\Gamma\rho_{\alpha, \alpha} = e\Gamma p_\alpha$ where $-e$ is the fundamental charge of an electron. The voltage across

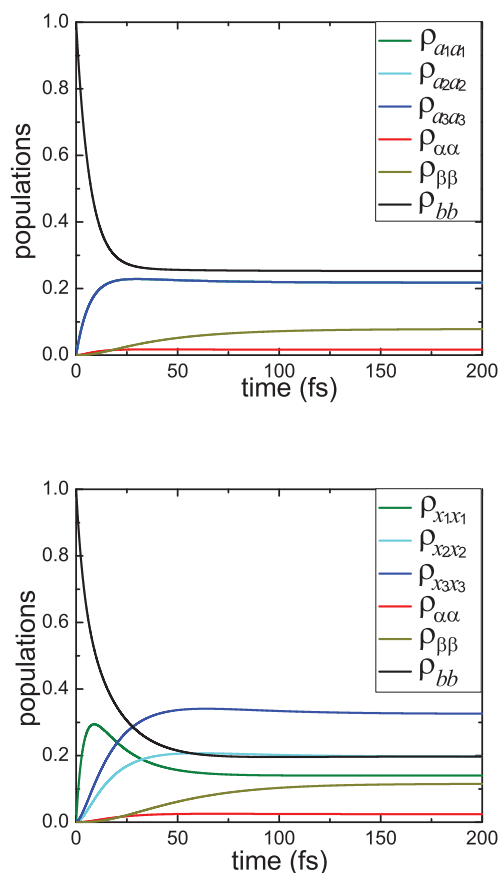


Fig. 5 (a) The time-evolutions of the populations p_i of the levels from the numerical solution of the Pauli master equation (Eq. 5) for uncoupled donors. (b) Numerical solutions of the Pauli master equation (Eq. 6) for coupled donors.

the solar cell is defined by the chemical potential difference between the two leads α and β , $eV \equiv e(V_\beta - V_\alpha) = \mu_\beta - \mu_\alpha$. Using the Boltzmann distributions for levels α and β , $p_\alpha = e^{-(E_\alpha - \mu_\alpha)/k_B T_a}$ and $p_\beta = e^{-(E_\beta - \mu_\beta)/k_B T_a}$, the voltage of the solar cell is expressed in terms of energy levels and populations^{20,24,34}.

$$eV = E_\alpha - E_\beta + k_B T_a \ln \left(\frac{p_\alpha}{p_\beta} \right). \quad (8)$$

The current and voltage are evaluated using the steady-state solutions of the PME.

Taking a modest recombination rate $\Gamma_{a \rightarrow b} = \chi\Gamma$ with $\chi = 20\%$, Fig. 6 shows the current enhancement as a function of the transition rate, γ_c , using the other parameters listed before. Under the upper limit condition, when $\gamma_c = \gamma_{12} = \gamma_{23}$, there is no current enhancement. This means that the charge

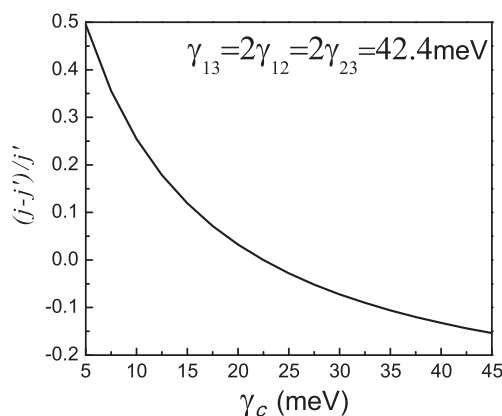


Fig. 6 Relative current enhancement $(j - j')/j'$ as a function of the transition rate γ_c between the donors and acceptor. Using the upper limit condition for γ_{12} , γ_{23} , and γ_{13} , we can get a current enhancement as high as 49.5%. On the other hand when $\gamma_c = \gamma_{12} = \gamma_{23}$, there is no current enhancement.

transfer via the channels $|x_1\rangle \rightarrow |\alpha\rangle$, $|x_1\rangle \rightarrow |x_3\rangle \rightarrow |\alpha\rangle$, and $|x_1\rangle \rightarrow |x_2\rangle \rightarrow |x_3\rangle \rightarrow |\alpha\rangle$ are as fast as the combined transfer through the independent channels $|a_1\rangle \rightarrow |\alpha\rangle$, $|a_2\rangle \rightarrow |\alpha\rangle$, and $|a_3\rangle \rightarrow |\alpha\rangle$. However, when $\gamma_c < \gamma_{12} = \gamma_{23}$, the coherent coupling leads to substantial current enhancements when compared to the configuration without coupling. Fig. 6 also shows that the current enhancement may reach as high as 49.5%, comparing this with 35% in Creatore *et al.*'s model. This can be explained by two factors: (i) the optical transition rate between the ground and the bright state is enhanced from 2 times to 2.9 times. (ii) the electron transition from the almost-dark (dark state in Ref.²⁴) to acceptor is increased from 2 times to 2.9 times. So a simple calculation shows the enhancement of PV model, $49.5\% \approx \frac{2.9}{2} \times 35\%$.

We have also explored the effect of the recombination rate, $\Gamma_{a \rightarrow b} = \chi\Gamma$, on the current enhancement. In Fig. 7, we show not only the current enhancement for the system comprised of three donors, (which is proposed here,) but also the current enhancement for the system with two donors, (that proposed in Ref.²⁴.) under similar electron transfer rate conditions. The results show that although the overall current is lower for faster recombination, the relative enhancement of the photocurrent is actually slightly larger for strong recombination. This behavior is analogous to that in the system with two donors²⁴. From Fig. 7, we also notice that the current enhancement in our three-donor system is much larger than that in Creatore *et al.*'s two-donor system at any value for the recombination rates. However, the current enhancement, on the order of 10^{-3} , from the two-coupled-donor model to the three-coupled-donor model is very small.

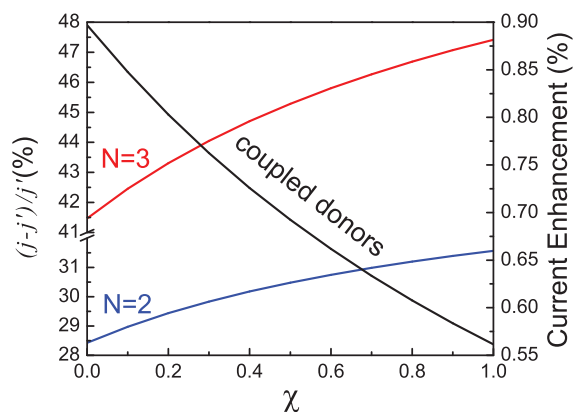


Fig. 7 Relative current enhancement $(j - j')/j'$ as a function of the recombination rate χ using $\gamma_c = 6$ meV. j and j' are the electric current in the excitonically coupled and uncoupled cases, respectively, when the system reaches steady-state operation. The red line represents the current enhancement for the system with three donors; the blue line represents the current enhancement for the system with two donors proposed by Creator *et al.*; the black line represents the current enhancement of our model comparing to Creator's model in the presence of dipolar coupling.

The current-voltage (j - V) characteristic at steady state is obtained by changing the rate Γ , while other parameters are fixed, from $\Gamma = 0$ (the open circuit regime where $j = 0$ and $V = V_{oc}$) to large Γ (the short circuit regime where $j \rightarrow j_{sc}$ and $V \rightarrow 0$). The power P is evaluated by the formula $P = j \cdot V$. Fig. 8 shows the steady-state current and power as a function of the voltage for three configurations of the donor: three uncoupled dipoles, two coupled dipoles, and three coupled dipoles. We find that the peak current of the solar cell with the three coupled dipoles ($J \neq 0$) increases by roughly 23.4% compared with the uncoupled three dipoles ($J = 0$). Consequently, the donor with the three coupled dipoles enhances the peak delivered power by about 23.0% relative to the uncoupled case. When compared to the two coupled dipole donor²⁴, also depicted in Fig. 8, the three coupled dipole donor has an enhancement of 6.3% in both peak current and peak delivered power.

One may wonder whether a donor with large N coupled dipoles could give rise to higher efficiency than two coupled dipoles²⁴ $N = 2$ or three coupled dipoles $N = 3$ studied here. Almost 60 years ago Dicke³² predicted the superradiance as the collective effect of N two-level atoms coupled with a radiation field. Recently Higgins *et al.*³³ proposed superabsorption of light via quantum engineering. This concept would be useful in enhancing the efficiency of the solar cell.

While the single donor-acceptor unit considered here shows

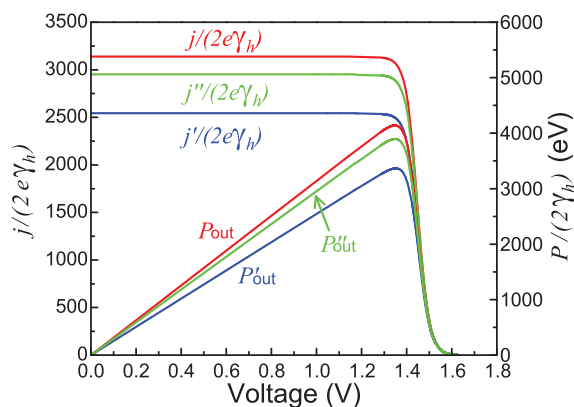


Fig. 8 Current j and power P_{out} as a function of the induced cell voltage V at room temperature for three configurations of donor dipoles. The blue lines and prime denote the case of three uncoupled dipoles ($J = 0$). The red lines represent the system with three coupled dipoles ($J \neq 0$). The green lines and double prime correspond to the case of two coupled dipoles²⁴.

high efficiency, a practical solar cell would be composed of a large number of inhomogeneous donor-acceptor units, so the overall enhancement could be affected. Specifically, all dipole molecules may neither be aligned in the same direction nor be equally spaced. One possible configuration is that donor k has the uniform coupling $J^{(k)} = J_{12}^{(k)} = J_{23}^{(k)}$ among three dipoles but it is different from donor to donor, $J^{(k)} \neq J^{(l)}$ for $k \neq l$. To calculate the ensemble average of the current-voltage characteristic, $J^{(k)}$ of the donor k could be sampled from the Gaussian distribution. In this case, the enhancement would be preserved because the energy level structure (dark, bright, and almost dark states) of each donor does not change. On the other hand, if three dipoles of each donor are coupled randomly, i.e., $J_{12}^{(k)} \neq J_{23}^{(k)}$, the excited states and the optical transition rate will be different from those of the uniform coupling case. Some donor-acceptor units with non-uniform dipole couplings would not show the high efficiency. To understand how the effects of inhomogeneous donor-acceptor units on the efficiency of the solar cell, one could do similar numerical calculations as done with the Heisenberg spin chain with random exchange couplings by Oh *et al.*³⁵

4 Conclusion

The study of photosynthesis has inspired a new method by which we may harness quantum effects and coherent coupling amongst chromophores for the formation of coherent superposition to realize an artificial light-harvesting system at the

molecular scale. In this paper, we propose a simple model to improve the performance of a theoretical photocell system. With suitably arranged electron donors, the photocurrents and power can be greatly enhanced through harnessing quantum effects.

The studied system is a photocell where the excitations are assumed resonant; for solar cells the excitation is done by solar radiation which has broad spectrum. However, the presented approach can be utilized in solar cells in different ways. One approach is to extend the system into N -dipole (extended bands) and use solar radiation for excitation. Another possibility is to host the dipole aggregates in solar cell materials close to the LUMO to suppress recombination and hence increase the collected photogenerated carriers³¹.

Developing new concepts to harvest and utilize energy based on lessons learned from nature like those in photosynthesis is of great current interest. Examining the current-voltage characteristic and power generated for the system with three coherent dipoles, we have found an efficiency enhancement of about 6.3% compared with two coherent dipoles. This encouraging trend suggest a promising novel design aspect of photosynthesis-mimicking photovoltaic devices.

References

- 1 G.S. Engel, T.R. Calhoun, E.L. Read, T.-K. Ahn, T. Mančal, Y.-C. Cheng, R.E. Blankenship, and G.R. Fleming, *Nature*, 2007, **466**, 782.
- 2 T.R. Calhoun, N.S. Ginsberg, G.S. Schlau-Cohen, Y.C. Cheng, M. Ballottari, R. Bassi, and G.R. Fleming, *J. Phys. Chem. B*, 2009, **113**, 16291.
- 3 D. Abramavicious, B. Palmieri, and S. Mukamel, *Chem. Phys.*, 2009, **357**, 79.
- 4 G. Panitchayangkoon, D. Hayes, K.A. Fransted, J.R. Caram, E. Harel, J. Wen, R.E. Blankenship, and G.S. Engel, *Proc. Natl. Acad. Sci. USA*, 2010, **107**, 12766.
- 5 E. Harel, A.F. Fidler, and G.S. Engel, *Proc. Natl. Acad. Sci. USA*, 2010, **107**, 16444.
- 6 D. Hayes, G.B. Griffin, and G.S. Engel, *Science*, 2013, **340**, 1431.
- 7 E. Romero, R. Augulis, V.I. Novoderezhkin, M. Ferretti, J. Thieme, D. Zigmantas, and R. van Grondelle, *Nat. Phys.*, 2014, **10**, 676.
- 8 M. Mohseni, P. Rebentrost, S. Lloyd, and A. Aspuru-Guzik, *J. Chem. Phys.*, 2008, **129**, 174106.
- 9 M.B. Plenio, and S.F. Huelga, *New J. Phys.*, 2008, **10**, 113019.
- 10 P. Rebentrost, M. Mohseni, I. Kassal, S. Lloyd, and A. Aspuru-Guzik, *New J. Phys.*, 2009, **11**, 033003.
- 11 J. Zhu and S. Kais, *J. Phys. Chem. B*, 2011, **115**, 1531.
- 12 S.-H. Yeh and S. Kais, *J. Chem. Phys.*, 2012, **137**, 084110.
- 13 W. Shockley and H.J. Queisser, *J. Appl. Phys.*, 1961, **32**, 510.
- 14 P. Würfel, *Physics of Solar Cells* (Wiley-VCH, Berlin, 2009).
- 15 *Quantum Efficiency in Complex Systems, Part II: From Molecular Aggregates to Organic Solar Cells* edited by U. Würfel, M. Thorwart, and, E. R. Weber, Semiconductors and Semimetals, Vol. 85 (Academic Press, San Diego, 2011).
- 16 O.D. Miller, E. Yablonovitch, and S.R. Kurtz, *IEEE J. Photovoltaics*, 2012, **2**, 303.
- 17 F.H. Alharbi, *J. Phys. D*, 2013, **46**, 125102.
- 18 F.H. Alharbi and S. Kais, *Renew. Sust. Energ. Rev.*, 2015, **43**, 1073.
- 19 R.E. Blankenship, D.M. Tiede, J. Barber, G.W. Brudvig, G. Fleming, M. Ghirardi, M.R. Gunner, W. Junge, D.M. Kramer, A. Melis, T.A. Moore, C.C. Moser, D.G. Nocera, A.J. Nozik, D.R. Ort, W.W. Parson, R.C. Prince, and R.T. Sayre, *Science*, 2011, **332**, 811.
- 20 M.O. Scully, *Phys. Rev. Lett.*, 2010, **104**, 207701.
- 21 M.O. Scully, K.R. Chapin, K.E. Dorfman, M.B. Kim, and A. Svidzinsky, *Proc. Natl. Acad. Sci. USA*, 2011, **108**, 15097.
- 22 A.A. Svidzinsky, K.E. Dorfman, and M.O. Scully, *Phys. Rev. A*, 2011, **84**, 053818.
- 23 K.E. Dorfman, D.V. Voronine, S. Mukamel, and M.O. Scully, *Proc. Natl. Acad. Sci. USA*, 2013, **110**, 2746.
- 24 C. Creatore, M.A. Parker, S. Emmott, and A.W. Chin, *Phys. Rev. Lett.*, 2013, **111**, 253601.
- 25 N. Killoran, S.F. Huelga, and M.B. Plenio, arXiv:1412.4136v1.
- 26 It should be noted that this efficiency may not be analogous to the Shockley Quisser limit¹³.
- 27 The Hamiltonian (2) is identical to an XY spin Hamiltonian. One exciton state corresponds to the one spin flipped state.
- 28 The single exciton eigenstates of Hamiltonian (2) are given explicitly as $|\pm\rangle = \frac{1}{\sqrt{2}}(|a_1b_2\rangle \pm |b_1a_2\rangle)$. For simplicity, these are written as $|\pm\rangle = \frac{1}{\sqrt{2}}(|a_1\rangle \pm |a_2\rangle)$.
- 29 H. van Amerongen, L. Valkunas, and R. van Grondelle, *Photosynthetic Excitons* (World Scientific, Singapore, 2000).
- 30 A. Shnirman, Y. Makhlin, and G. Schön, *Phys. Scr.*, 2002, **T102**, 147.
- 31 S.K. Saikin, A. Eisfeld, S. Valleau, and A. Aspuru-Guzik, *Nanophotonics*, 2013, **2**, 21.
- 32 R.H. Dicke, *Phys. Rev.*, 1954, **93**, 99.
- 33 K.D.J. Higgins, S.C. Benjamin, T.M. Stace, G.J. Milburn, B.W. Lovett, and E.M. Gauger, *Nature Comms.*, (2014), DOI:10.1038/ncomms5705.

-
- 34 If instead of the Boltzmann distribution, the Fermi-Dirac distribution $p_\alpha = \frac{1}{\exp[(E_\alpha - \mu_\alpha)/k_B T] + 1}$ is used, the voltage formula will be modified as $eV = E_\alpha - E_\beta + k_B T_a \ln \left[\frac{p_\alpha(1-p_\beta)}{p_\beta(1-p_\alpha)} \right]$. This gives rise to a slightly different I - V characteristics.
- 35 S. Oh Y.-P. Shim, J. Fei, M. Friesen, and X. Hu, *Phys. Rev. B*, 2012, **85**, 224418.